Supplementary Information for

Climate-driven oscillation of phosphorus and iron limitation in the North Pacific Subtropical Gyre

Ricardo M. Letelier, Karin M. Björkman, Matthew J. Church, Douglas S. Hamilton, Natalie M. Mahowald, Rachel A. Scanza, Niklas Schneider, Angelicque E. White, and David M. Karl

Corresponding authors: Ricardo M. Letelier & David M. Karl
Emails: letelier@oregonstate.edu & dkarl@hawaii.edu

This PDF file includes:

www.pnas.org/cgi/doi/10.1073/pnas.1900789116

Fig. S1.

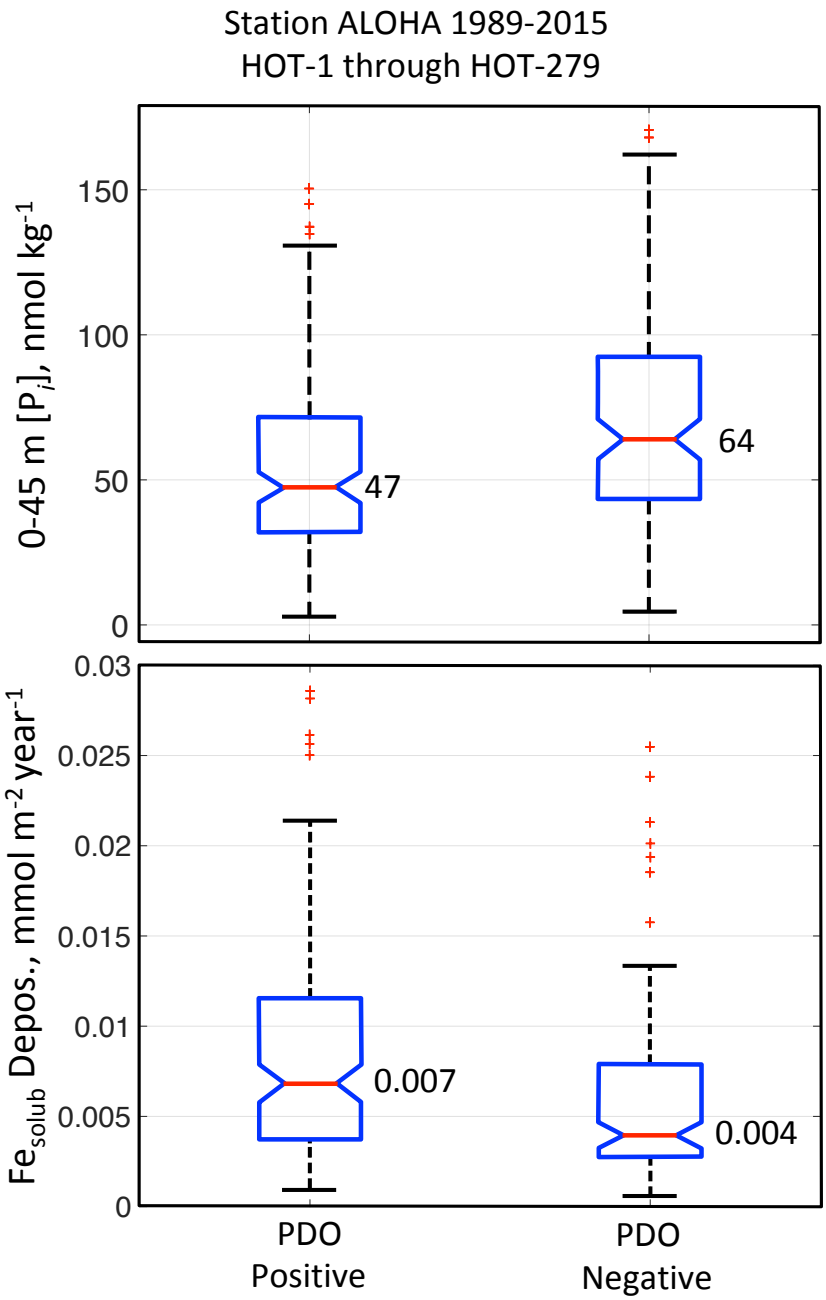

Box-and-Whisker plots displaying the median, standard error of the median (box notches), 25th and 75th percentile of 0–45 m depth P_i concentration observed at Station ALOHA (upper panel) and model derived soluble Fe deposition (lower panel) during positive and negative PDO periods.

Fig. S2.

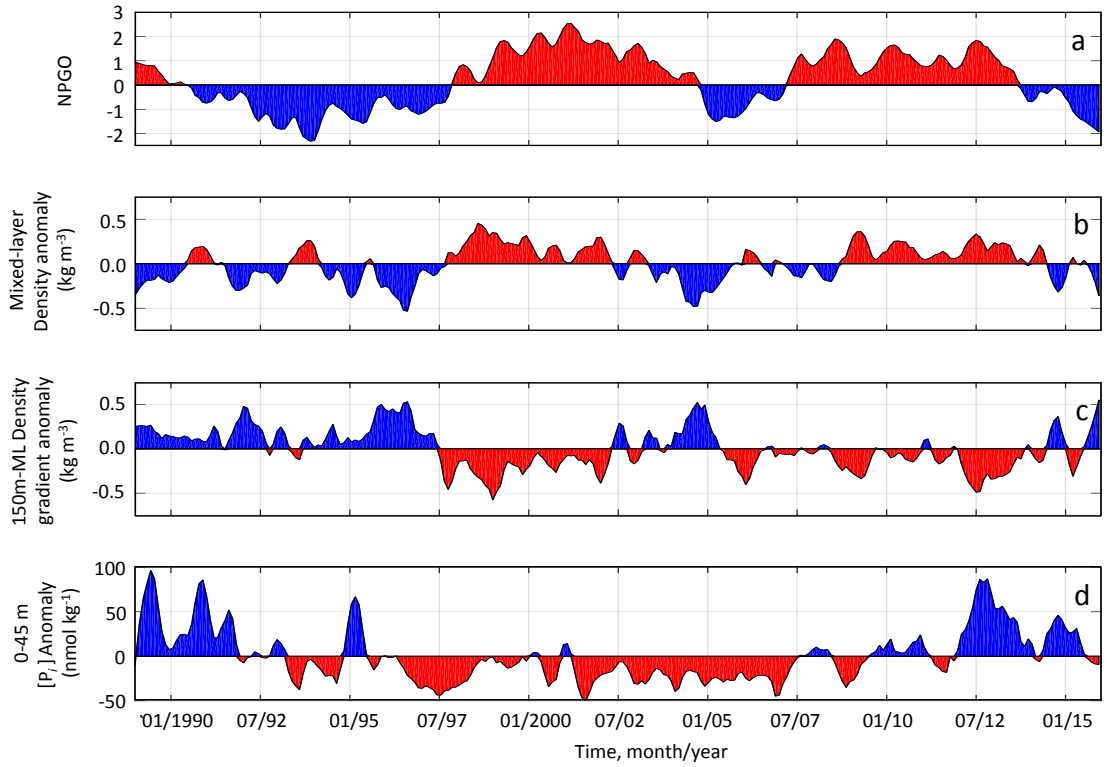

Time-series of a) the North Pacific Gyre Oscillation (NPGO) Index, b) Mixed-layer Density anomaly, c) Upper water column 0- to 150-m gradient anomaly, and d) 0-45 m depth mean P_i concentration anomaly. All anomalies correspond to residuals following the removal of the mean seasonal climatology.

Fig. S3.

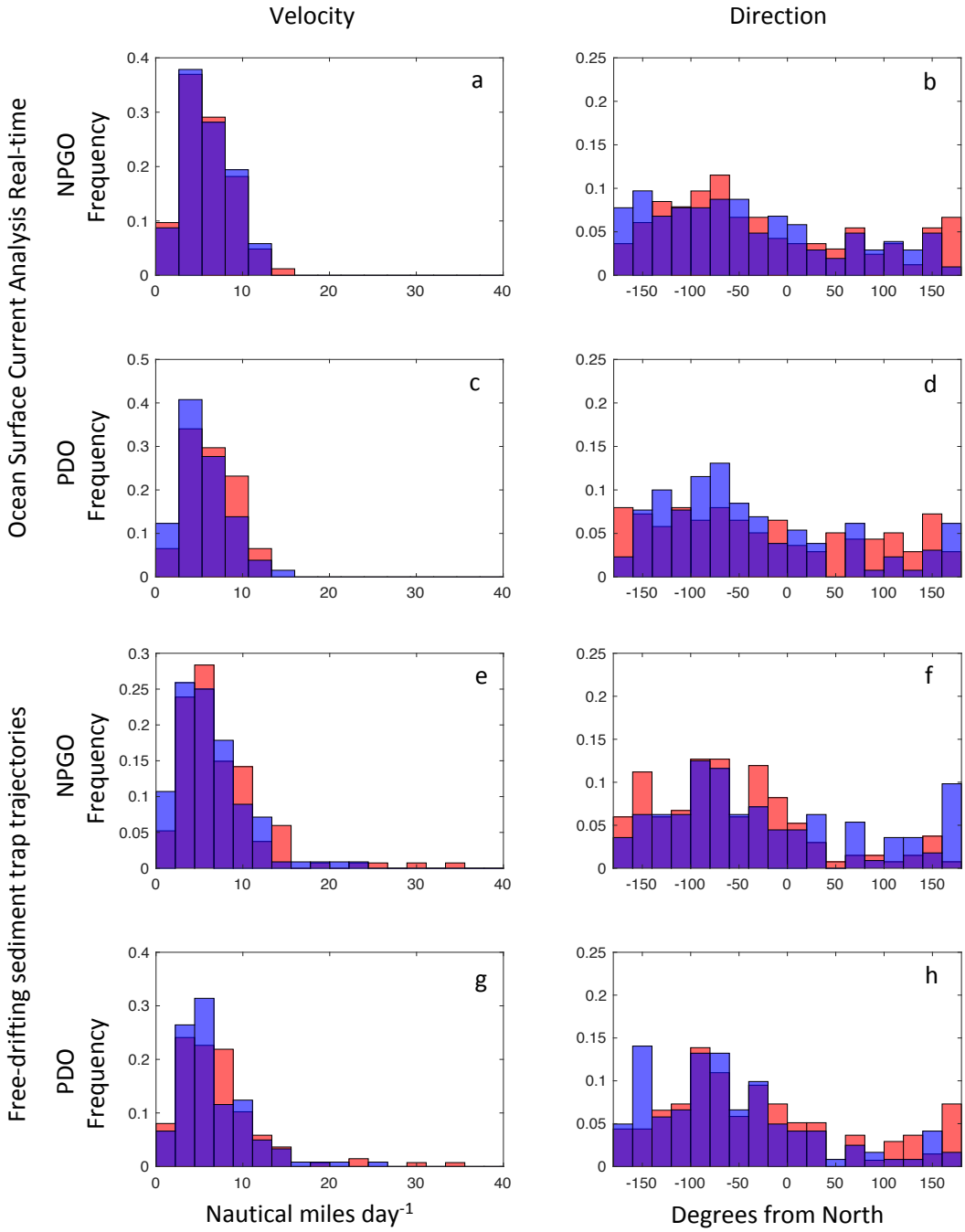

Comparison of the frequency distributions of ocean surface currents velocity (left column) and direction (right column) as a function of positive (red) and negative (blue) climate index conditions. (a, b, e and f = NPGO; c, d, g and h = PDO). Values derived from the Tropical Ocean Surface Current Analysis Real-time (OSCAR) model (1) for the region 158.2°W-156.2°W and 22.2°N–24.2°N (upper four panels) and from the drift of sediment traps deployed during HOT cruises (lower four panels).

Fig. S4.

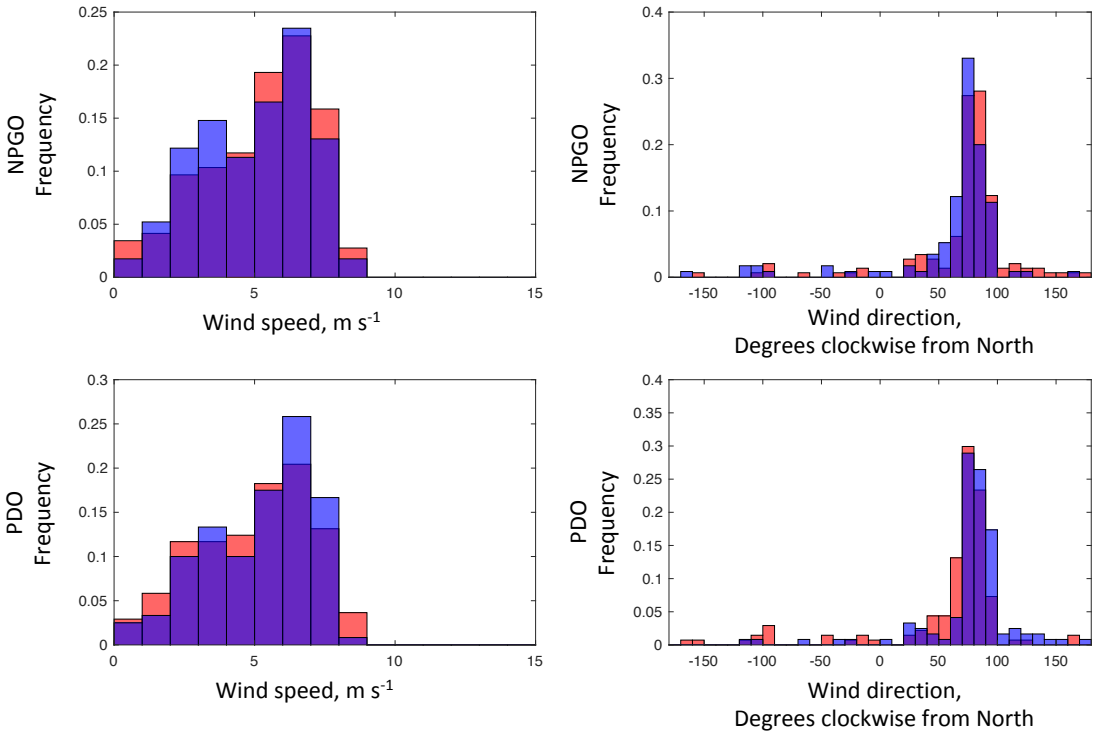

Comparison of the distributions of monthly mean wind speed and direction recorded by the NDBC buoys 51001 and 51101 between January 1989 and December 2015 as a function of positive (red) and negative (blue) climate index conditions.
Upper panels = NPGO, lower panels = PDO.

Fig. S5.

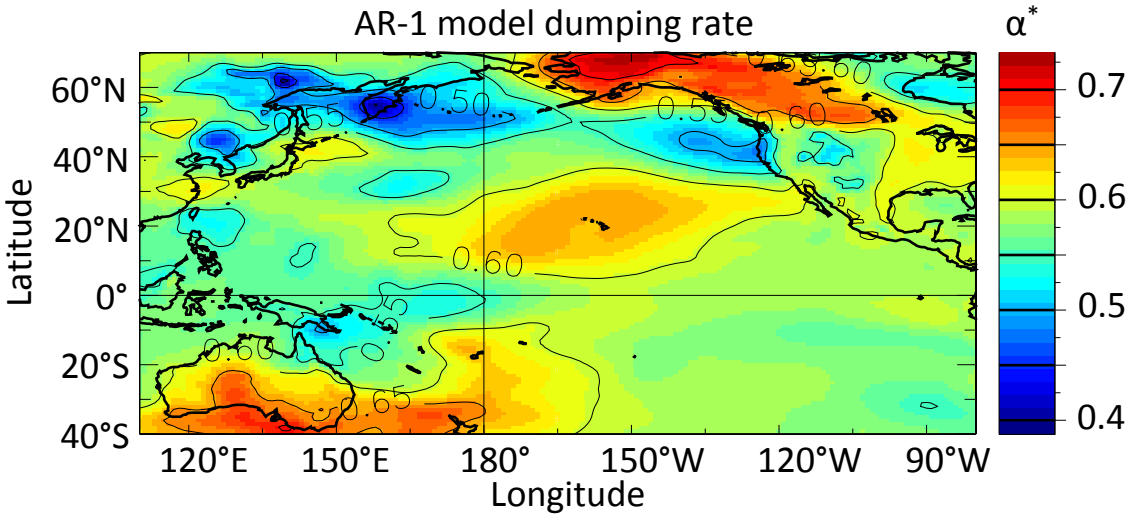

Spatial distribution of the damping rate $\alpha^* = 1 - \alpha \Delta t$ (see Equation 1), where α corresponds to the damping time scale in years.

Fig. S6.

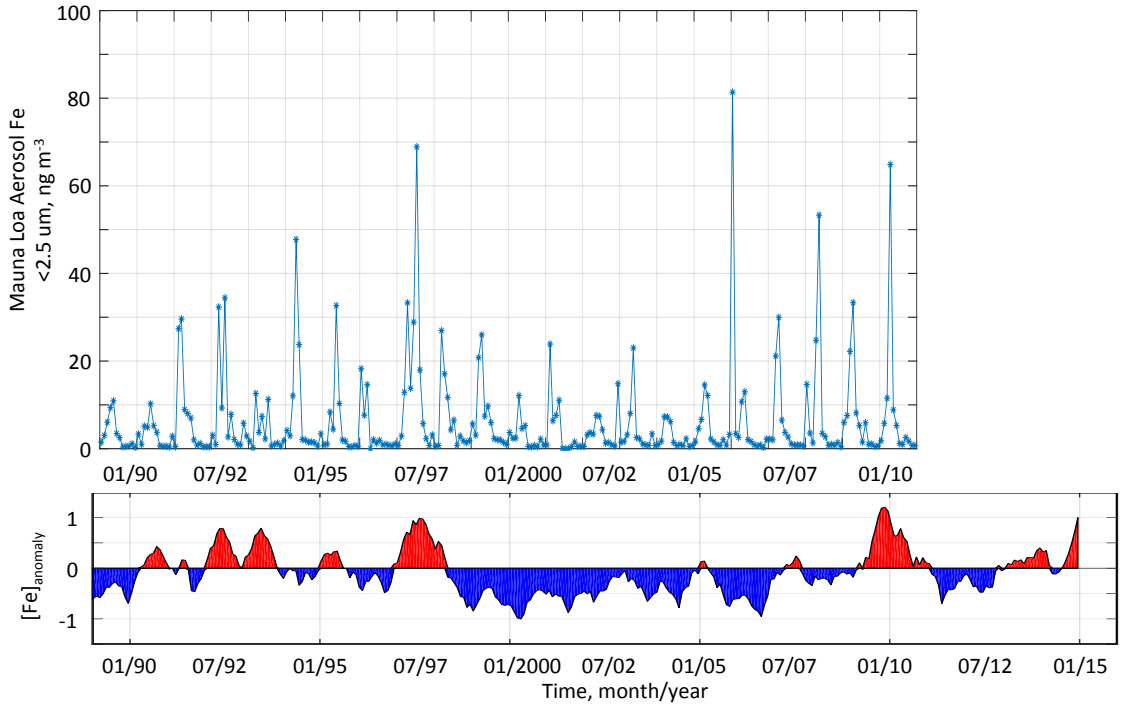

Time-series of (upper panel) monthly mean atmospheric aerosol Fe (<2.5 μm) collected at Mauna Loa Observatory between January 1989 and December 2010 (2) and (lower panel) seasonally de-trended and standardized model-derived atmospheric Fe dust concentration.

Fig. S7.

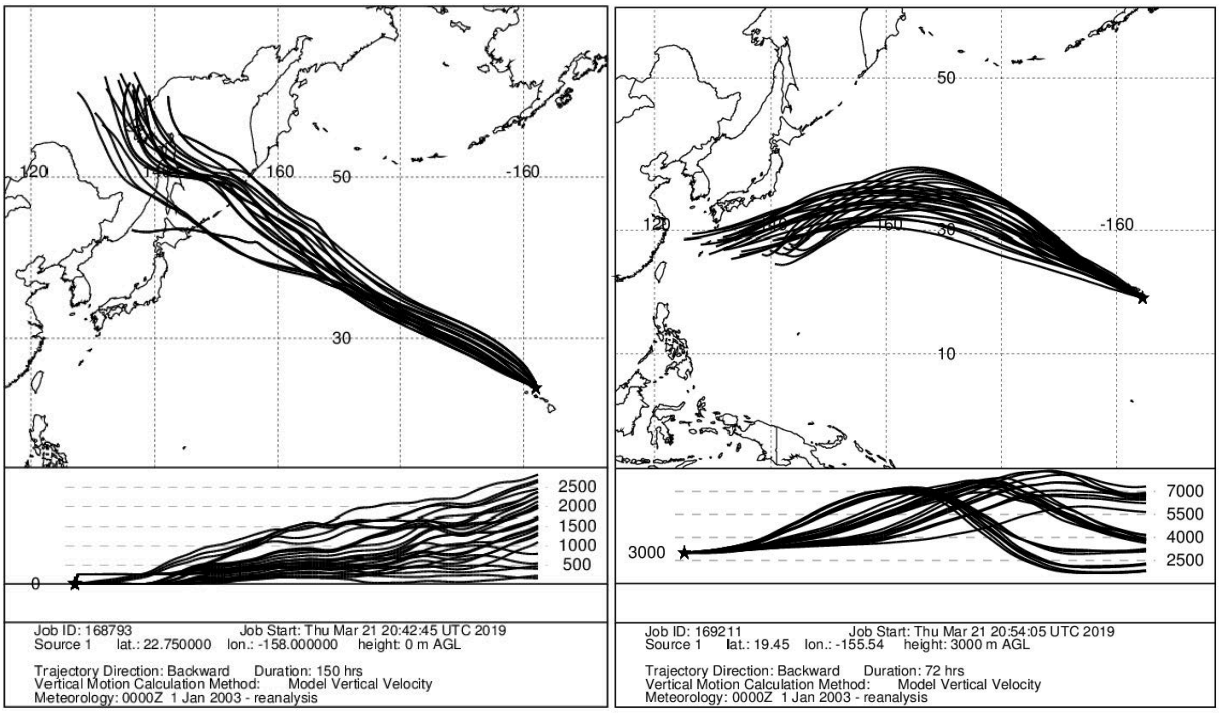

Comparison of 150 hours backtrack atmospheric particle ensemble trajectories reaching Station ALOHA (left panel) and the Mauna Loa Observatory (right panel) on January 1st 2003. Analysis based on NCEP/NCAR reanalysis using NOAA's HYSPLIT Atmospheric Transport and Dispersion Modeling System (3).

Table S1. Changes in the mean (± S.E.M.) mixed-layer condition observed at Station ALOHA during different phases of the PDO and NPGO. Anomalies are based on residuals following the removal of the 1989-2015 seasonal climatology. Statistical significance based on 1-way ANOVA.

	PDO (+)	PDO (-)	Significance p <	NPGO (+)	NPGO (-)	Significance p <
0-45 m $[P_i]$ (nmol kg^{-1})	54.1 ± 2.6	72.5 ± 3.7	**0.001**	64.7 ± 3.1	59.9 ± 3.2	ns
0-45 m $[NO_3^- + NO_2^-]$ (nmol kg^{-1})	4.1 ± 0.2	4.2 ± 0.1	n.s.	3.9 ± 0.1	4.4 ± 0.2	**0.05**
$Fe_{solub.}$ Deposition rate (µmol m^{-2} y^{-1})	9.8 ± 0.7	6.2 ± 0.4	**0.001**	7.0 ± 0.7	7.0 ± 0.6	n.s.
Mixed-Layer Temperature anomaly (°C)	0.11 ± 0.05	-0.13 ± 0.05	**0.001**	-0.07 ± 0.04	0.09 ± 0.05	**0.05**
Mixed-Layer Salinity anomaly (o/oo)	-0.032 ± 0.015	0.037 ± 0.017	**0.01**	0.056 ± 0.014	-0.071 ± 0.017	**0.001**
Mixed-Layer to 150m Density gradient anomaly (kg m^{-3})	0.081 ± 0.025	-0.085 ± 0.021	**0.001**	-0.081 ± 0.023	0.086 ± 0.023	**0.001**
0-45 m chl *a* anomaly (mg m^{-3})	-0.004 ± 0.002	0.005 ± 0.003	**0.05**	0.004 ± 0.003	-0.006 ± 0.002	**0.01**
0-45 m Primary Production anomaly (mg C m^{-3})	-0.114 ± 0.132	0.070 ± 0.162	ns	0.109 ± 0.144	-0.204 ± 0.134	ns
0-45 m Assimilation number anomaly (mg C [mg chl *a* $hr]^{-1}$)	0.125 ± 0.156	-0.129 ± 0.142	ns	-0.060 ± 0.138	0.092 ± 0.167	ns

References

1. Bonjean F, Lagerloef GSE (2002) Diagnostic model and analysis of the surface currents in the tropical Pacific Ocean. *J Phys Ocean* 32:2938-2954.
2. Hyslop NP, Trzepla K, Wallis CD, Matzoll AK, White WH (2013) Technical note: A 23-year record of twice-weekly aerosol composition measurements at Mauna Loa Observatory. *Atmos Environ* 80:259-263.
3. Stein AF, Draxler RR, Rolph GD, Stunder BJB, Cohen MD, Ngan F (2015) NOAA's HYSPLIT Atmospheric transport and dispersion modeling system. *Bull Amer meteor Soc* 96: 2059-2077.